# The effect of environment on the radial breathing mode of supergrowth single wall carbon nanotubes

Cite as: Appl. Phys. Lett. **95**, 261902 (2009); https://doi.org/10.1063/1.3276909
Submitted: 08 October 2009 . Accepted: 03 December 2009 . Published Online: 28 December 2009

P. T. Araujo, C. Fantini, M. M. Lucchese, M. S. Dresselhaus, and A. Jorio

# The effect of environment on the radial breathing mode of supergrowth single wall carbon nanotubes

P. T. Araujo,[1,a] C. Fantini,[1] M. M. Lucchese,[2] M. S. Dresselhaus,[3] and A. Jorio[1,2]
[1]*Departamento de Física, Universidade Federal de Minas Gerais, Belo Horizonte, Minas Gerais 30123-970, Brazil*
[2]*Divisão de Metrologia de Materiais, Instituto Nacional de Metrologia, Normalização e Qualidade Industrial (INMETRO), Duque de Caxias, Rio de Janeiro 25250-020, Brazil*
[3]*Department of Electrical Engineering and Computer Science and Department of Physics, Massachusetts Institute of Technology, Cambridge, Massachusetts 02139-4307, USA*

(Received 8 October 2009; accepted 3 December 2009; published online 28 December 2009)

It has been shown that "supergrowth" single wall carbon nanotubes (SWNTs) exhibit a radial breathing mode frequency $\omega_{RBM}$ dependence on tube diameter $d_t$ given by $\omega_{RBM}=227/d_t$. This result gave rise to two distinct scenarios for SWNTs: one for the supergrowth radial breathing mode and another for all the other samples reported in the literature. Here we show that, by dispersing the supergrowth SWNTs in surfactant or bringing them into interacting bundles, it is possible to merge these two scenarios, where now the supergrowth SWNT properties are similar to all SWNT properties reported so far in the literature. © *2009 American Institute of Physics*. [doi:10.1063/1.3276909]

Because of its direct relation to the SWNT diameter ($d_t$), the radial breathing mode frequency ($\omega_{RBM}$) has become the most important spectroscopic signature of single wall carbon nanotubes (SWNTs).[1,2] Together with information about its optical transition energies ($E_{ii}$), the $\omega_{RBM}$ leads to the assignment of the SWNTs $(n,m)$ indices.[1,2] Recently, the relation $\omega_{RBM}=227/d_t$ was found for the so-called "supergrowth" SWNTs,[1] which is a notable result because of the following: (1) it is in accordance with elasticity theory and tight-binding calculations, parameterized by the speed of sound in graphite;[3,4] (2) it recovers the graphene sheet limit where $\omega_{RBM}\rightarrow 0$ when $d_t\rightarrow\infty$; (3) it represents the lowest $\omega_{RBM}$ value reported so far.[1] This result gave rise to two different scenarios: one for the supergrowth $\omega_{RBM}$ and another for all the other values reported in the literature, which were shown to be fitted by $\omega_{RBM}=(227/d_t)\sqrt{1+C_e\times d_t^2}$. The reason why[1] only the supergrowth sample exhibits the unique properties listed under points (1) and (2) is still not yet understood. The purpose of the present letter is to show that, if the supergrowth material is dispersed in some surfactant environment or brought into interacting bundles, the supergrowth $\omega_{RBM}$ behaves like all the SWNTs in the literature, following exactly the same van der Waals interaction model described in Ref. 1. This new result provides additional evidence that these supergrowth SWNTs are somehow shielded from interactions with the environment.

Resonance Raman spectroscopy was used to study the $\omega_{RBM}$ of the supergrowth SWNTs under three different conditions as follows: (I) as an as-grown carpetlike sample, (II) in a solution, dispersed with a surfactant, and (III) in bundles. The dispersion of supergrowth SWNTs was prepared in an aqueous solution of sodium dodecyl sulfate (SDS). A SWNT concentration of 0.05 mg/mL with 1 wt % surfactant was prepared in de-ionized water. A volume of 6 mL was sonicated for 30 min using an ultrasonic tip probe at a power level of 10 W. After sonication, the suspensions were centrifuged at 20 800g for 60 min. The bundled sample was obtained after drying the dispersion supernatant residual on a microscope coverslip. Micro-Raman scattering measurements were performed with a Horiba Jobin–Ivon T64000 triple-monochromator equipped with a $N_2$ cooled charge coupled device detector, in the backscattering configuration. Previously measured Raman maps, constructed by using different excitation laser energies,[2,5–8] are here used as a guide for the $(n,m)$ analysis which can be shown here by employing a single laser line. The excitation laser energy chosen for this experiment was the most commonly found in worldwide laboratories, $E_{laser}=2.41$ eV (514.5 nm). The laser power density was maintained constant, at a low enough power level to avoid heating effects (20 mW in the solution sample and 0.43 mW in the bundled and as-grown samples). In the solution sample, the laser beam was focused with a 50 ×microscope objective while in the bundled and as-grown samples a 100×microscope objective was employed.

Figure 1(a) gives the Raman spectrum obtained from the supergrowth SWNTs in SDS solution (top), the Raman spectrum obtained from the bundled sample (middle) and the Raman spectrum from the as-grown supergrowth SWNTs (bottom). All of these spectra are normalized to the highest intensity peak. By comparing the spectra in Fig. 1(a) it is clear that the surfactant dramatically suppresses the Raman response of tubes with diameters higher than 0.9 nm ($d_t\geq 0.9$ nm) when in solution. When drying the bundled sample, the RBM response for tubes with diameters ranging from 0.9 to 1.3 nm is recovered. This result is consistent with experiments of absorption, photoluminescence, and Raman scattering in other SWNTs samples.[9–14] To quantify the changes in the RBM frequencies due to a changing environment, Fig. 1(b) shows the spectra presented in Fig. 1(a) zoomed into the frequency range 150 to 300 $cm^{-1}$. In each spectrum, the raw spectra are fitted by Lorentzians representing SWNTs that are in resonance and contribute to the spectra. Table I summarizes the frequencies and $(n,m)$ indices of the tubes assigned in each spectrum. The arrows in the figure

[a]Electronic mail: pauloata@fisica.ufmg.br.

 

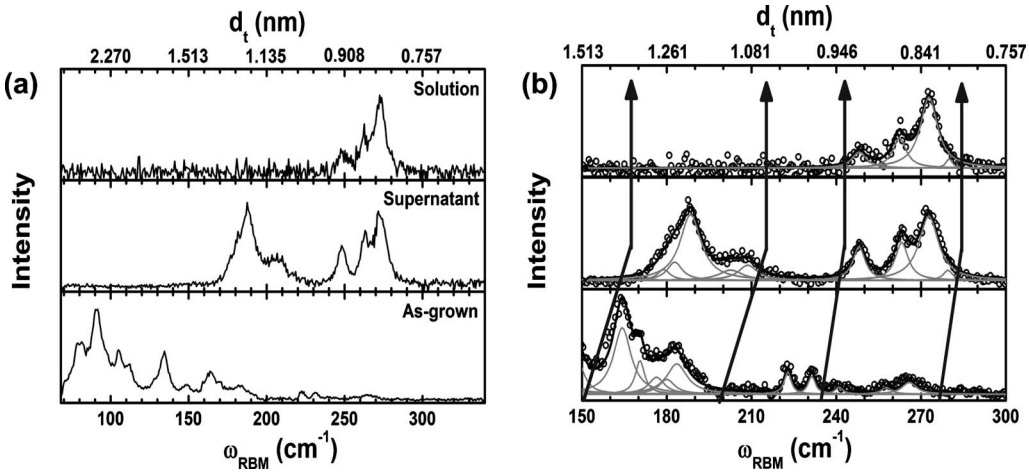


FIG. 1. (a) The Raman spectrum obtained from: (top) the solution of supergrowth SWNTs@SDS, (middle) the bundled sample and (bottom) the as-grown supergrowth sample. All the spectra were obtained by using $E_{laser}=2.41$ eV (514.5 nm) and normalized to the highest intensity peak. (b) Spectra presented in Fig. 1(a) zoomed into the frequency range 150 to 300 $cm^{-1}$. The open circles represent the raw data and the solid gray curves are Lorentizians representing the RBMs from the SWNT species in resonance. The black solid line is the result obtained from the Lorentizian fitting procedure. The arrows are a guide to the eyes showing that the $\omega_{RBM}$ is upshifted for the solution and bundled samples. Furthermore, wrapping and bundling change the SWNT optical properties (Ref. 8). Therefore, relative RBM intensities change and some SWNTs that are in resonance in the as-grown sample are not in resonance in the solution and bundled samples.

serve as a guide to the eyes, whereby we can easily realize that the frequencies for the solution and bundled samples, which from now on are called, respectively, $\omega_{RBM}^{solut.}$ and $\omega_{RBM}^{bundl.}$, are upshifted with respect to the as-grown values $\omega_{RBM}^{as\text{-}grown}$. In agreement with what is reported in Ref. 1, the larger the $d_t$ value, the higher is the frequency upshift. No difference is observed between the $\omega_{RBM}^{solut.}$ and the $\omega_{RBM}^{bundl.}$, which suggests that the interactions between the tubes with their respective environments are in the same range of strength.

Figure 2 shows the differences between $\omega_{RBM}^{solut./bundl.}$ and $\omega_{RBM}^{as\text{-}grown}$ plotted as a function of $d_t$. The open circles stand for $\Delta\omega_{RBM}^{bundl.}=\omega_{RBM}^{bundl.}-\omega_{RBM}^{as\text{-}grown}$ and the down triangles stand for $\Delta\omega_{RBM}^{solut.}=\omega_{RBM}^{solut.}-\omega_{RBM}^{as\text{-}grown}$ (see Table I). The inset shows the measured $\omega_{RBM}$ as a function of $1/d_t$. The black solid line in Fig. 2, which fits the symbols, is given by $\Delta\omega_{RBM}^{solut./bundl.}=\omega_{RBM}^{solut./bundl.}-\omega_{RBM}^{as\text{-}grown}=227/d_t[\sqrt{1+C_e\times d_t^2}-1]$, with $C_e=0.056$. This is basically the same curve as was obtained in Ref. 1, where $C_e=0.057$. This result shows that now the $\omega_{RBM}$ for both solution and bundled samples follow exactly the same van der Waals interaction model that describes all the $\omega_{RBM}$ values in the literature. Therefore, by exposing the supergrowth SWNTs to a surfactant and bundling, changing its natural environment, we could merge their radial breathing mode scenario with the scenario of all SWNTs in the literature.[1]

In summary, we have used resonance Raman spectroscopy to study the supergrowth SWNTs dispersed with sodium dodecyl sulfate (SDS) in two situations as follows: (1) in solution and (2) in bundles, formed after drying the supernatant solution residual. The $\omega_{RBM}$ for both solution and bundles are upshifted in relation to the frequencies observed in the as-grown sample, following exactly the same van-der-Waals interaction model that describes all the $\omega_{RBM}$ in the literature.[1] Finally, while the as-grown supergrowth SWNTs have tubes whose frequencies are described by $\omega_{RBM}^{as\text{-}grown}=227/d_t$, the frequencies for the tubes in solution and in bundles are described by $\omega_{RBM}^{solut./bundl.}=(227/d_t)\sqrt{1+C_e\times d_t^2}$, with $C_e=0.056$.

TABLE I. $\omega_{RBM}$ values and respective $(n,m)$ assignments for the as-grown, solution, and bundled SWNTs. Here $\Delta\omega_{RBM}^{solut./bundl.}=\omega_{RBM}^{solut./bundl.}-\omega_{RBM}^{as\text{-}grown}$.

| $\omega_{RBM}^{as\text{-}grown}$ | $\omega_{RBM}^{bundl.}$ | $\omega_{RBM}^{solut.}$ | $(n,m)$ | $\Delta\omega_{RBM}^{bundl.}$ | $\Delta\omega_{RBM}^{solut.}$ |
|---|---|---|---|---|---|
| 275.1[a] | 279.5 | 279.9 | (10,1) | 4.4 | 4.9 |
| 267.1 | 272.8 | 272.8 | (9,3) | 5.6 | 5.7 |
| 257.6 | 263.2 | 262.3 | (8,5) | 5.6 | 4.7 |
| 240.9 | 248.0 | 248.0 | (7,7) | 7.1 | 7.1 |
| 222.8 | 228.0[b] | 228.0[b] | (9,6) | 5.2 | 5.2 |
| 199.5[a] | 208.7 | 206.6[b] | (14,1) | 9.2 | 7.1 |
| 196.7[a] | 202.7 | 203.9[b] | (13,3) | 5.9 | 7.2 |
| 183.6 | 188.9[b] | 188.9[b] | (16,0) | 5.3 | 5.3 |
| 180.4 | 188.4 | 187.9[b] | (15,2) | 8.0 | 7.5 |
| 176.2 | 182.9 | 185.0[b] | (14,4) | 6.7 | 8.8 |
| 170.5 | 178.7 | 180.4[b] | (13,6) | 8.3 | 10.0 |
| 164.8 | 173.7 | 174.7[b] | (12,8) | 8.9 | 9.9 |

[a]Calculated using $\omega_{RBM}=227/d_t$.
[b]Calculated using $\omega_{RBM}=(227/d_t)\sqrt{1+0.056\times d_t^2}$.

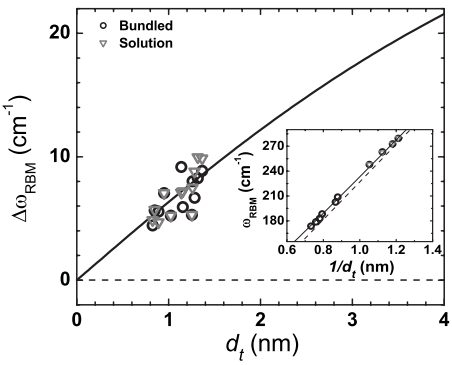


FIG. 2. The as-grown supergrowth frequencies ($\omega_{RBM}^{as\text{-}grown}$) are subtracted from the frequencies of both solution (▽) and bundled (○) samples represented, respectively, by $\omega_{RBM}^{solut.}$ and $\omega_{RBM}^{bundl.}$, and plotted as function of $d_t$. The solid curve describes the frequency shift behavior due to van der Waals interactions between the tube walls and their environment, as described in Ref. 1. Inset: $\omega_{RBM}^{solut./bundl.}$ plotted as a function of $1/d_t$, where the dashed line is given by $\omega_{RBM}^{as\text{-}grown}=227/d_t$ and the solid line is given by $\omega_{RBM}^{solut./bundl.}=(227/d_t)\sqrt{1+0.056\times d_t^2}$.

P.T.A. and A.J. acknowledge financial support from the Brazilian agency CNPq and from the American agency AFOSR/SOARD (Award No. FA9550-08-1-0236). M.S.D. acknowledges support from NSF Grant No. DMR07-04197. C.F. acknowledge financial support from CNPq Grant No. 479007/2008-0.

[1]P. T. Araujo, I. O. Maciel, P. B. C. Pesce, M. A. Pimenta, S. K. Doorn, H. Qian, A. Hartschuh, M. Steiner, L. Grigorian, K. Hata, and A. Jorio, Phys. Rev. B **77**, 241403(R) (2008).
[2]A. Jorio, M. S. Dresselhaus, and G. Dresselhaus, *Carbon Nanotubes: Advanced Topics in the Synthesis, Structure, Properties, and Applications*, Springer Series on Topics in Appl. Phys. Vol. 111 (Springer, Berlin, 2008).
[3]G. D. Mahan, Phys. Rev. B **65**, 235402 (2002).
[4]V. N. Popov and P. Lambin, Phys. Rev. B **73**, 085407 (2006).
[5]H. Telg, J. Maultzsch, S. Reich, F. Hennrich, and C. Thomsen, Phys. Rev. Lett. **93**, 177401 (2004).
[6]C. Fantini, A. Jorio, M. Souza, M. S. Strano, M. S. Dresselhaus, and M. A. Pimenta, Phys. Rev. Lett. **93**, 147406 (2004).
[7]P. T. Araujo, S. K. Doorn, S. Kilina, S. Tretiak, E. Einarsson, S. Maruyama, H. Chacham, M. A. Pimenta, and A. Jorio, Phys. Rev. Lett. **98**, 067401 (2007).
[8]P. T. Araujo and A. Jorio, Phys. Status Solidi B **245**, 2201 (2008).
[9]A. Jorio, A. P. Santos, H. B. Ribeiro, C. Fantini, M. Souza, J. P. M. Vieira, C. A. Furtado, J. Jiang, R. Saito, L. Balzano, D. E. Resasco, and M. A. Pimenta, Phys. Rev. B **72**, 075207 (2005).
[10]S. Giordani, S. D. Bergin, V. Nicolosi, S. Lebedkin, M. M. Kappes, W. J. Blau, and J. N. Coleman, J. Phys. Chem. B **110**, 15708 (2006).
[11]C. Fantini, A. Jorio, A. P. Santos, V. S. T. Peressinotto, and M. A. Pimenta, Chem. Phys. Lett. **439**, 138 (2007).
[12]D. A. Tsyboulski, E. L. Bakota, L. S. Witus, J.-D. R. Rocha, J. D. Hartgerink, and R. B. Weisman, J. Am. Chem. Soc. **130**, 17134 (2008).
[13]S. D. Bergin, V. Nicolosi, H. Cathcart, M. Lotya, D. Rickard, Z. Sun, W. J. Blau, and J. N. Coleman, J. Phys. Chem. C **112**, 972 (2008).
[14]C. Fantini, J. Cassimiro, V. S. T. Peressinotto, F. Plentz, A. G. Souza Filho, C. A. Furtado, and A. P. Santos, Chem. Phys. Lett. **473**, 96 (2009).